Effect of physical distancing on the speed–density relation in pedestrian dynamics

I Echeverría-Huarte[1,*], A Garcimartín[1], D R Parisi[2], R C Hidalgo[1], C Martín-Gómez[3] and I Zuriguel[1]

[1] Departamento de Física y Mat. Apl., Facultad de Ciencias, Universidad de Navarra, E-31080 Pamplona, Spain
[2] Instituto Tecnológico de Buenos Aires (ITBA) CONICET, Lavardén 315, (1437) C A de Buenos Aires, Argentina
[3] Departamento de Construcción, Instalaciones y Estructuras, Escuela Técnica Superior de Arquitectura, Universidad de Navarra, E-31080 Pamplona, Spain
E-mail: iecheverria.13@unav.es

Abstract. We report experimental results of the speed–density relation emerging in pedestrian dynamics when individuals keep a prescribed safety distance among them. To this end, we characterize the movement of a group of people roaming inside an enclosure varying different experimental parameters: (i) global density, (ii) prescribed walking speed, and (iii) suggested safety distance. Then, by means of the Voronoi diagram we are able to compute the local density associated to each pedestrian, which is afterward correlated with its corresponding velocity at each time. In this way, we discover a strong dependence of the speed–density relation on the experimental conditions, especially with the (prescribed) free speed. We also observe that when pedestrians walk slowly, the speed–density relation depends on the global macroscopic density of the system, and not only on the local one. Finally, we demonstrate that for the same experiment, each pedestrian follows a distinct behavior, thus giving rise to multiple speed–density curves.

Keywords: traffic and crowd dynamics

Contents

1. Introduction

Over the last three decades, the study of pedestrian dynamics has provided a theoretical and experimental framework that has been essential for the design and management of public areas. Evaluating the movement of pedestrians in different situations has become vitally important, helping to prevent accidents when large crowds gather, for instance in music concerts, sport events or commercial centers. Since the pioneering work of Helbing *et al* [1], experiments and numerical models have been developed and used to create safer building codes [2–4]. Most of them focus on evaluating the capacity of a system in terms of flow, speed and density, in order to avoid reaching values that could endanger people safety.

One of the most broadly accepted empirical notions used to predict pedestrian behavior is the so-called fundamental diagram (FD). Initially proposed for the study of traffic [5], it relates the flow with the density. The notion is that when the number of vehicles in a road grows above a critical density value, the flow rate is reduced. Following this approach, the use of FD as a way to study the capacity of collective systems was widely adopted and it started to be used in pedestrian dynamics. Nowadays, the FD is one of the most important macroscopic observables used in this field [6–11] allowing to establish comparisons between different experiments and validating numerical models. Furthermore, the FD has been applied in different scenarios and geometries, such as waiting rooms, stairs, sidewalks, or corridors with uni and bidirectional pedestrian flow [12].

A sound alternative to the flow vs density relation is representing the speed vs density curve [13–20]. Both methods are equivalent since the flux or specific flow rate (i.e. the flow per unit length) of a system is nothing else than the speed times the density. However, the interpretation offered by the speed–density relation is more straightforward. Indeed, it typically reveals that people's speed decrease as the density (number of pedestrians) in a system increases. Different works have characterized this relation

in several ways. Older [14], Fruin [21] and Tanaboriboon [22] obtained a linear dependence between both magnitudes, studying the cases of shopping streets, bus terminals and sidewalks respectively. Virkler and Elayadath [23] found that the best model to fit the curve was an exponential form with different parameters depending on the density. Finally, Buchmüller and Weidmann [12] approximated the speed–density diagram with the so called Kladek formula. It establishes that, for low densities, the speed is independent of this magnitude (it presents a plateau for low densities). Then, beyond a certain density (around 0.5 ped m^{-2}) the speed starts decreasing. Interestingly, the speed value observed at low densities can be interpreted as the desired speed that pedestrians will have when they do not interact with other people.

Nowadays, due to the impact of the COVID-19 outbreak, the way people move has drastically changed. After authorities have prescribed a social distance of around 1.5 m (this number varies depending on the country), pedestrian dynamics in public spaces has been modified. Therefore, it is necessary to understand and quantify this transformation. Some of the first studies have begun evaluating the distance between people by means of computer simulations [24, 25] and field measurements [26]. In [24], Parisi *et al* examined how safety distance was affected by increasing the number of people within an ideal supermarket. Studying pedestrians' trajectories, they measured the number of events in which a prescribed safety distance (PSD) of 2 m was infringed and for how long. Besides, a social distance coefficient was defined in order to obtain a criterion that might be used as a guide for establishing reasonable capacities of such locations. Their findings suggest that, depending on the allowed exposure time, the maximum densities should range from 0.02 to 0.2 ped m^{-2}. Mayr and Köster [25] focused on bottlenecks, providing an update for the optimal steps model to simulate social distancing in the pedestrian dynamics simulator *Vadere*. In particular, they carried out a systematic study of two of the model's parameters: the personal space breadth and the repulsion potential height, finding the set of values that were most suitable to respect the imposed social distance. Finally, Pouw *et al* [26] worked with video recordings taken at a train station. They compared the pre-epidemic and current scenarios, estimating physical distances and exposure times via a sparse graph. As well as offering a useful tool for pedestrian identification in real-time, their study included the detection of family groups; in this way, they were able to measure the actual social distance between individuals (or groups).

Also, we have recently investigated this topic by means of controlled lab experiments [27]. In these tests, a number of people gathered in an enclosure and were asked to roam at different speeds while keeping a PSD of 2 or 1.5 m depending on the experiment. Our findings revealed that global densities should not be higher than 0.16 pedestrians per square meter (around 6 square meters per pedestrian) in order to guarantee an interpersonal distance of, at least, 1 m. Surprisingly, we also evidenced a dual role of increasing walking speed (WS). On one hand, it caused more events where the PSD was not respected but, on the other hand, it facilitated a quicker resolution of these conflicts. Finally, we proved the importance of prescribing an ample safety distance as some people may likely underestimate the actual value of the interpersonal distance.

All the studies mentioned above have mainly focused on examining the link between some variables (density, velocity, ...) and the parameters that are believed to be related

to the propagation of COVID-19 (e.g. interpersonal distance or exposure times). However, to our knowledge none of them study how the relationship between these variables changes after imposing a social distancing. In order to fill this gap, we extend our previous research and present a novel analysis of the speed–density relation. Note that in our scenario the flow pattern is multidirectional, meaning that there is not a preferred walking direction. This situation attempts to mimic the usual walking patterns at open spaces such as a marketplace or a wide sidewalk, among others.

2. Experimental setup and data processing

The experiment took place in a University building on 23 June 2020. Prior to its implementation, all security protocols related to the sanitary circumstances at that time were accepted by the University of Navarra ethics committee. Thus, a total of 38 people (28 men and 10 women) aged between 19 to 59 years participated in the experiment which was conducted for 3 h approximately. During this time, all participants had to wear a mask and use hydro-alcoholic gel in order to respect the sanitary rules imposed.

In the experiment, different number of people were asked to stroll inside an enclosure at different stipulated WS while keeping a PSD of either 2 or 1.5 m, depending on the test. For the purpose of checking the reproducibility of the experiments, each experimental condition was repeated twice with different people. To this end, each volunteer was given an ID-card with a number, in order to summon a particular subset to participate in each experiment. In this way, a total of 24 runs were performed for 12 different experimental conditions. The instructions given to the participants were rather simple: they were asked to roam within the arena keeping the PSD and avoiding stopping as much as possible. For the case of slow walking they were asked to roam peacefully, as if they were window shopping in a street with no rush at all. For the case of fast walking, they were just asked to walk fast, without further explanation.

The enclosure was 11.4 m wide by 6.7 m long and was delimited by 90 cm high tables. Four doors allowed the entry and exit of pedestrians (figure 1(a)). Once inside the arena, participants had to take as their starting position one of the spots marked with a cross on the ground (see marks in figure 1(a)). These points had been previously set at 2 m or 1.5 m depending on the PSD so as to make sure that all participants initially respected this condition. Besides, these marks served as a reference for participants to estimate the distance they had to keep.

Once everybody had occupied their initial positions, a sound signal marked the experiment start. Each round consisted of three random movement phases (of 40 s duration each) where people were asked to walk freely respecting the PSD. These three phases were interspersed with two periods of movement toward the walls, in attempt to prevent the emergence of organized collective movements. In [27], a more detailed description of the experiment as well as an example of the trajectories followed by pedestrians—to check the homogeneous occupation of space—can be found. As in that work, only the random motion stage will be considered in this study.

All experiments were recorded with a 4k resolution camera located 12 m above the enclosure at a frame-rate of 25 fps. Using a reference checker board, all videos were

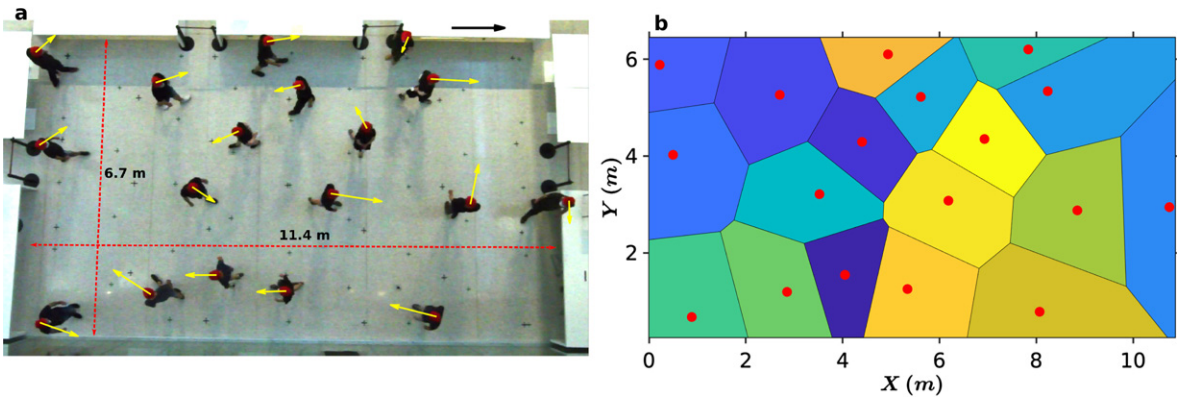

Figure 1. (a) Snapshot of an experiment carried out with 18 people walking at a slow pace for a prescribed safety distance (PSD) of 1.5 m. In the floor, the different crosses mark the initial positions adopted by pedestrians. They were arranged equidistantly at 2 m (black spots) or 1.5 m (green spots) depending on the PSD of the experiment. Yellow arrows denote the instantaneous velocities of each pedestrian based on the scale indicated by the black vector located at the top right of the panel (1 m s^{-1}). (b) The Voronoi diagram has been calculated from (a), taking into account the edge restrictions of the finite system. The Voronoi cells corresponding to each pedestrian have been given different colors. In this way, the area A_i for each pedestrian can be obtained, and thus the corresponding individual density ρ_i.

corrected from camera tilting (image distortion was negligible) in order to perform an accurate detection of the pedestrians' positions. From these, we obtained the trajectories and velocities of each pedestrian (figure 1(a)) as well as the corresponding Voronoi diagrams (figure 1(b)). The later, were used to calculate the individual densities at the location of each pedestrian as the inverse of their Voronoi areas. Both the speed values and the Voronoi diagrams were calculated over a sliding window of 0.76 s in order to obtain records where the system would present a different arrangement of pedestrians. Thus, every 0.76 s, a list of speed–density values associated with each pedestrian was obtained. With these data, a study of speed–density relation was carried out taking into account not only averaged magnitudes over all pedestrians but also the individual relation associated to each individual.

Finally, it is important to note that due to the boundary conditions imposed on our experimental system, one should be cautious when extrapolating our results to more realistic scenarios. In real life, the role played by other variables (such as walking in groups, stationary people waiting for someone, mixture of fast and slow walking people) in the emerging pedestrian dynamics is quite important and, in our study, these effects have not been contemplated. However, since there are no previous experimental studies where the effect of social distancing on the speed–density relation has been investigated, we believe that this work can be used as a first approach for characterizing systems where a safe interpersonal distancing has been requested.

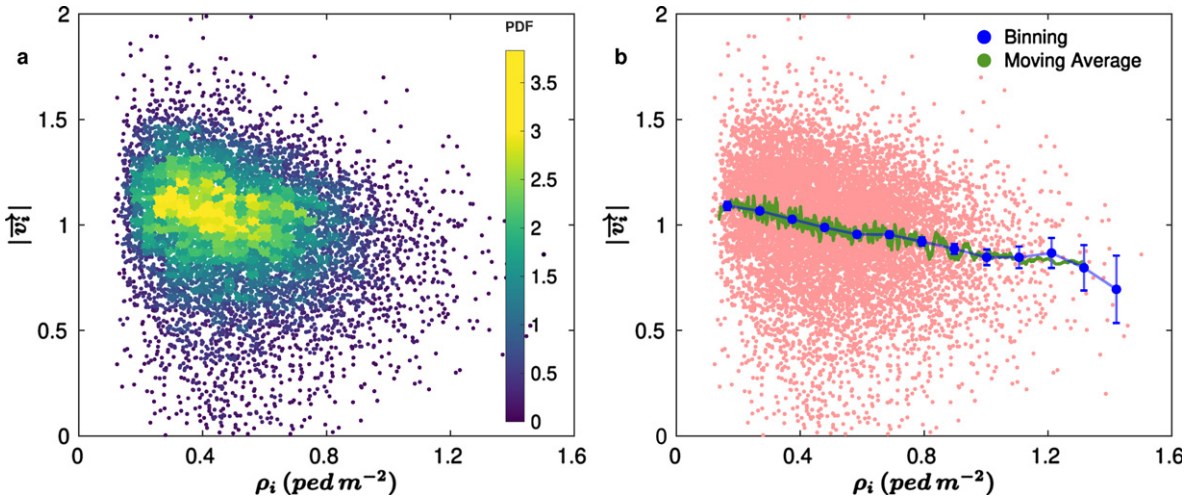

Figure 2. Speed–density relation for an experiment with 32 pedestrians walking at a slow pace with a PSD of 1.5 m. Each dot (same in both graphs) represents the pair of values $[|\vec{v}_i|, \rho_i]$ registered for each pedestrian at a time t. (a) The 2D PDF has been computed as explained in the text. Then, each dot is colored based on the normalized frequency as shown in the colorbar. (b) The blue line shows the average $|\vec{v}_i|$ value calculated by clustering the data into bins of $\Delta\rho = 0.1\,\text{ped m}^{-2}$. Error bars have been computed as the standard error with a confidence level of 95%. The green line depicts a moving average of the data over a sliding window which length is 100 data points.

3. Results

In figure 2, the speed–density relation is displayed for a single experiment (32 pedestrians with slow WS and a PSD of 1.5 m). Since each experimental condition was repeated twice, the graph shows the whole statistics considering both runs. Thus, each dot in the plot represents a single measure of $|\vec{v}_i|$ and ρ_i for a specific pedestrian at a given time. Therefore, the dot cloud is the total number of single records taken during both replicates. First of all, let us point out that the recorded density values were quite low if we compare them with other experiments where the speed–density relation has been studied [16–19]. This was expected as given the pandemic circumstances the global density in the experiment was quite small in all cases. That said, aiming for a better characterization of the data, a bivariate histogram has been computed in figure 2(a) by clustering the data in square boxes with side length 0.04. Then, each box has been divided by its area and the total number of data, thus obtaining a correct normalisation of the histogram. Most of the density data fall between 0.3 and 0.5 ped m^{-2} (see yellowish colors in the colorbar); in this region it seems that a slight decreasing of $|\vec{v}_i|$ takes place as ρ_i increases. In order to corroborate this trend, the dependence between $|\vec{v}_i|$ and ρ_i has been studied (figure 2(b)) in two ways: (i) by clustering the data into bins of $\Delta\rho = 0.1\,\text{ped m}^{-2}$ and then calculating their mean values and error bars as the standard error with a confidence level of 95%; and (ii) by calculating a moving average over a sliding window of length $k = 100$ points. As expected from figure 2(a), both methods

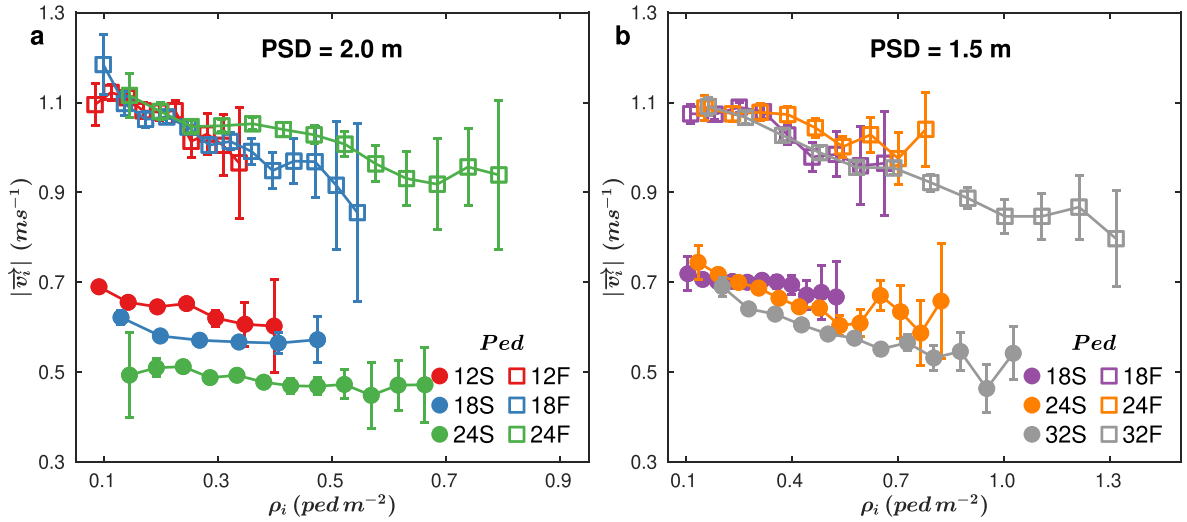

Figure 3. Mean speed–density diagrams for all trials. Each panel displays the experiments carried out with a PSD of: (a) 2.0 m and (b) 1.5 m. Color codes the number of pedestrians inside the arena, while the markers (circles or squares) indicate the WS at which the volunteers were asked to walk (slow, S, and fast, F).

reveal a decreasing tendency in $|\vec{v}_i|$ as the density increases. Since the trend of the data is largely similar regardless of the methodology chosen, we will present only the first method from now on for simplicity.

Once we have checked that we can precisely define the speed–density relation from the individual data, in figure 3 we represent the specific curve for each experimental condition investigated. Figures 3(a) and (b) correspond to a PSD of 2.0 and 1.5 m respectively (see plot headings). Let us first analyze figure 3(a), where the decreasing trend in $|\vec{v}_i|$ as ρ_i increases is observed once again regardless of the experimental condition. Remark that the increase of error bars in $|\vec{v}_i|$ when ρ_i grows is due to the smaller number of data corresponding to higher densities. This is caused by the imposed PSD, which prevents people from getting too close to each other. Therefore, high density values (small Voronoi areas) are statistically underrepresented.

The effect of the stipulated WS on the speed–density relation is notable. Slow and fast WS result in two different groups of speed–density diagrams. This is quite interesting, because it proves that the dynamics of the system is not completely determined by geometry, density and other physical constraints; the desired velocity of pedestrians, all other things being equal, will result in a different speed–density relation. Therefore this variable (or a similar one) should be included in the description of the experimental conditions.

Let us now focus on a feature that arises when the global density of the system (number of people within the enclosure) varies. For slow WS and a PSD of 2 m, a gap between curves can be observed: as the number of pedestrian within the arena increases, the velocity reduces. This tendency is not observed for the fast WS experiments, for which all curves overlap. We guess that, when imposing a big safety distance and slow WS, pedestrians have the ability to take into account not only their first neighbors (those

who surround their Voronoi area), but also some other people farther away. Importantly, this result implies that the global density of the system (and not only the local one) is relevant for the dynamics of individual pedestrians. As the speed of the volunteers increases, they find themselves too busy trying to avoid close approaches, which makes it impossible for them to take into account the position of distant pedestrians. In this case, the effect of the global density does not influence the dynamics, causing the overlap between the curves for different densities at high WS.

Concerning the effect of the PSD, we observe that the speed–density diagram for 1.5 m (figure 3(b)) is similar to the one for 2.0 m (figure 3(a)). Probably the most salient difference is that the variation—if any—caused by different global densities for slow WS is much smaller when the PSD is 1.5 m. If the above hypothesis is correct, this would make sense as by reducing the PSD, the individual pedestrian dynamics would be dominated by the business of collision avoidance, and it would more likely be restricted to their first neighbors.

In order to check that the motion of pedestrians walking slow and with an imposed safety distance of 2 m is affected by the global density (and not only the local one), we represent in figure 4 the outcomes from the two runs implemented for each experimental condition. Even though the data dispersion is a little bit more important than in figure 3(a) (as the number of data used to build each single curve is halved) the difference among the three density–speed relationships is still clear. This corroborates the finding reported in figure 3(a), and supports the idea that the global perception of pedestrians has an effect on the dynamics, when the values of PSD are high and the WS is slow.

So far, it is quite remarkable how experimental conditions (including, as we stated above, not only density and PSD, but also the stipulated WS) have distinct effects in the speed–density relations. Therefore, one could ponder whether or not these speed–density ratios are also different at the individual level (considering each pedestrian separately). In other words, we wonder if in our conditions, each pedestrian behaves following their own speed–density relationship. Since data on individual pedestrians were available over a long period of time, it is possible to obtain individual speed–density relations for each pedestrian, as shown in figures 5(a) and (b). In this case, two different experiments with a PSD of 2.0 m are depicted (see panel headings for experimental conditions). It can be observed by looking at colored lines that most of the people have associated curves that systematically lie either above or below the mean curve (black line). This seems to indicate that it is not the result of statistical variability but it hints instead to the existence of different attitudes taken by pedestrians during the same experiment. Aiming to confirm this trend, pedestrians are separated in two groups according to their average speed values when the density is very low (i.e. when it is smaller than $0.1\,\mathrm{ped\,m^{-2}}$). We split pedestrians in two categories, fast or slow, depending on whether their $|\vec{v}_i|$ values at very low densities are greater or smaller than the mean. The reason behind this procedure hinges on the fact that speed at low density can be interpreted as an individual desired speed [12]. It can be appreciated from figures 5(c) and (d) that both fast and slow pedestrians systematically maintain the same trend as the density increases. Fast pedestrians always lie above the average curve, and slow ones remain below. This corroborates that our system not only has a different speed–density relation

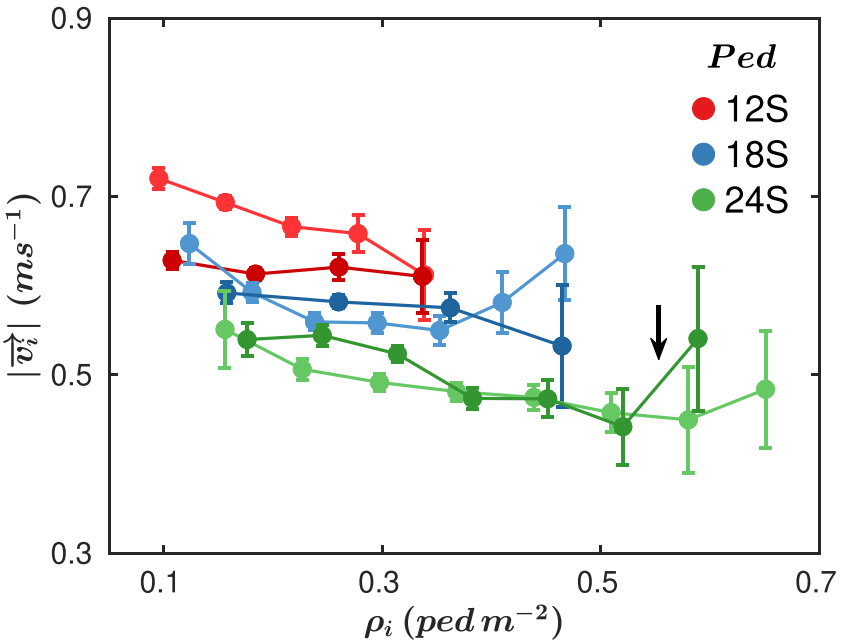

Figure 4. speed–density diagrams for each single run carried out at slow WS and PSD = 2.0 m. The curve annotated with a black arrow corresponds to a single experiment conducted with 23 people (instead of 24) due to an experimental error. The data for this case have been only used to plot this figure and are not included in figure 3.

depending on the experimental conditions but also that, within the same experiment, different attitudes coexist among pedestrians.

Finally, in order to highlight the differences between pedestrians, the probability density functions (PDFs) of ρ_i and $|\vec{v}_i|$ are depicted in figures 5(e)–(h) for each individual. Pedestrians and color lines are the same as in figures 5(a) and (b). Regarding ρ_i, no big differences are appreciated between individuals and the global PDF curves (figures 5(e) and (g)). For the $|\vec{v}_i|$ case (figures 5(f)–(h)), the differences between individuals are more pronounced. Again, we have pedestrians whose distributions' mean values are either shifted to the left or to the right compared with the overall distribution. In any case, for both ρ_i and $|\vec{v}_i|$ it can be seen that the distributions are wider for the case of 24 pedestrian moving fast than for 12 pedestrians moving slowly.

Now, in order to better quantify how the ρ_i and $|\vec{v}_i|$ distributions change for different individuals, we will take the average of the individual PDFs as a descriptor. Thus, we define $\langle \rho_i \rangle_P$ and $\langle |\vec{v}_i| \rangle_P$ as the time averages of these magnitudes for each pedestrian. Then, the boxplots of both averages are computed and shown in figures 6(a), (b), (d) and (e). All experiments are represented, coding them as AB_C, being A the number of pedestrians (12, 18, 24, 32) inside the arena, B the WS (S for slow and F for fast) and C

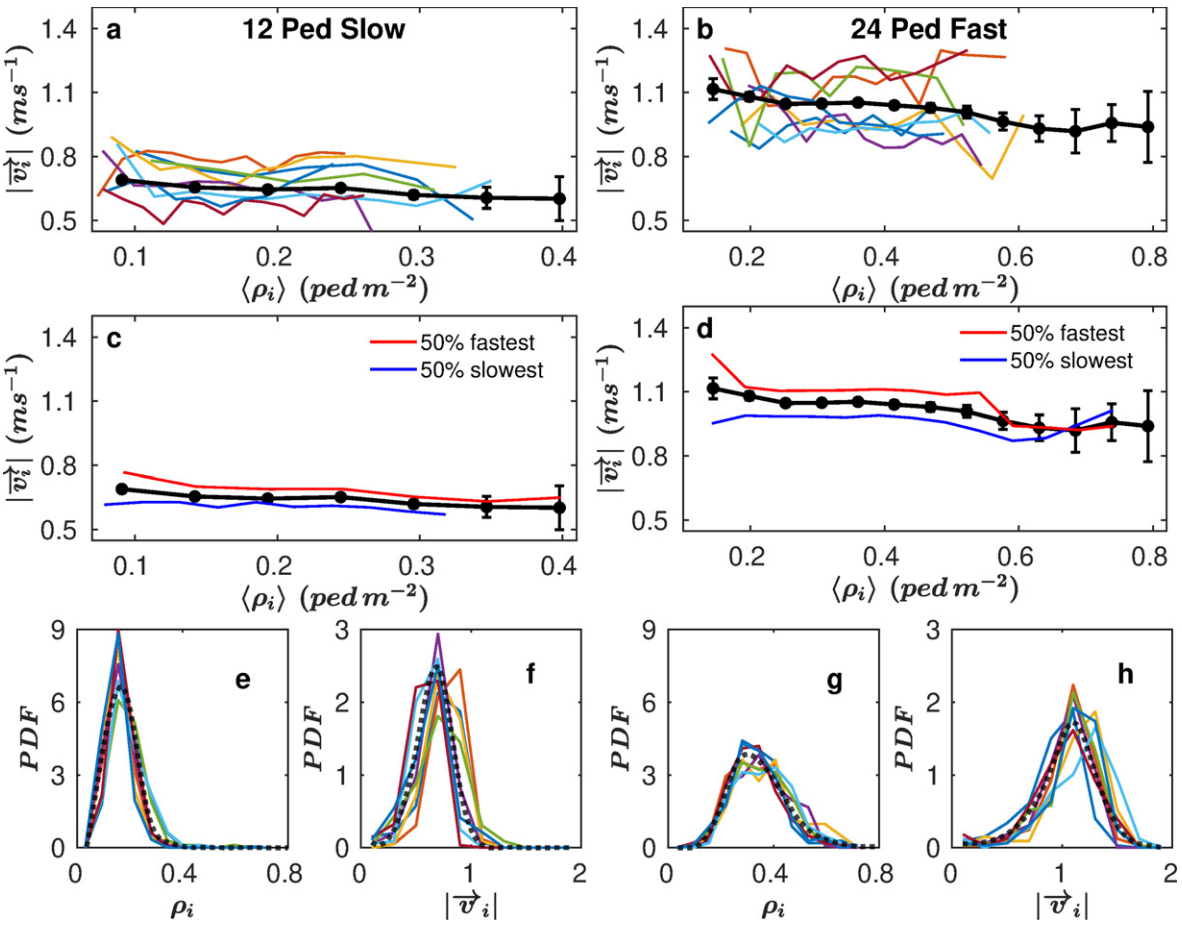

Figure 5. Individual speed–density relations and PDFs for ρ_i and $|\vec{v}_i|$. The graphs in each column correspond to different experimental conditions as indicated in the upper headings of (a) and (b). In both cases, the PSD was 2 m. (a), (b) Individual speed–density curves have been calculated for each pedestrian. For clarity, only the curves of eight pedestrians have been plotted. Black solid lines are the mean speed–density relation as in figure 3(a). (c), (d) The speed–density relation has been recalculated by grouping pedestrians according to their $|\vec{v}_i|$ value in the region of very low ρ_i values: those whose speed is higher than the average (red) and those whose speed is lower (blue). (e), (g) PDFs of ρ_i values. (f), (h) the PDFs for $|\vec{v}_i|$. The same pedestrians and color lines as in (a) and (b) are represented. (e) and (f) correspond to 12 pedestrians walking slow, whereas (g) and (h) to 24 pedestrians walking fast. Black dotted lines represent the global PDFs using all data.

the PSD (2.0 or 1.5 m). For instance, $12S_{2.0}$ denotes an experiment with 12 pedestrians at a slow WS and with a PSD of 2.0 m.

Starting with the values of $\langle\rho_i\rangle_P$ (figures 6(a) and (b)), it seems that the dispersion increases (the differences among individuals become more important) as the global density (number of pedestrians inside the enclosure) grows. On the contrary, the dispersion seems to remain more or less unchanged when comparing slow with fast cases and PSD $= 2$ with PSD $= 1.5$ m (given that the global density is the same). Perhaps,

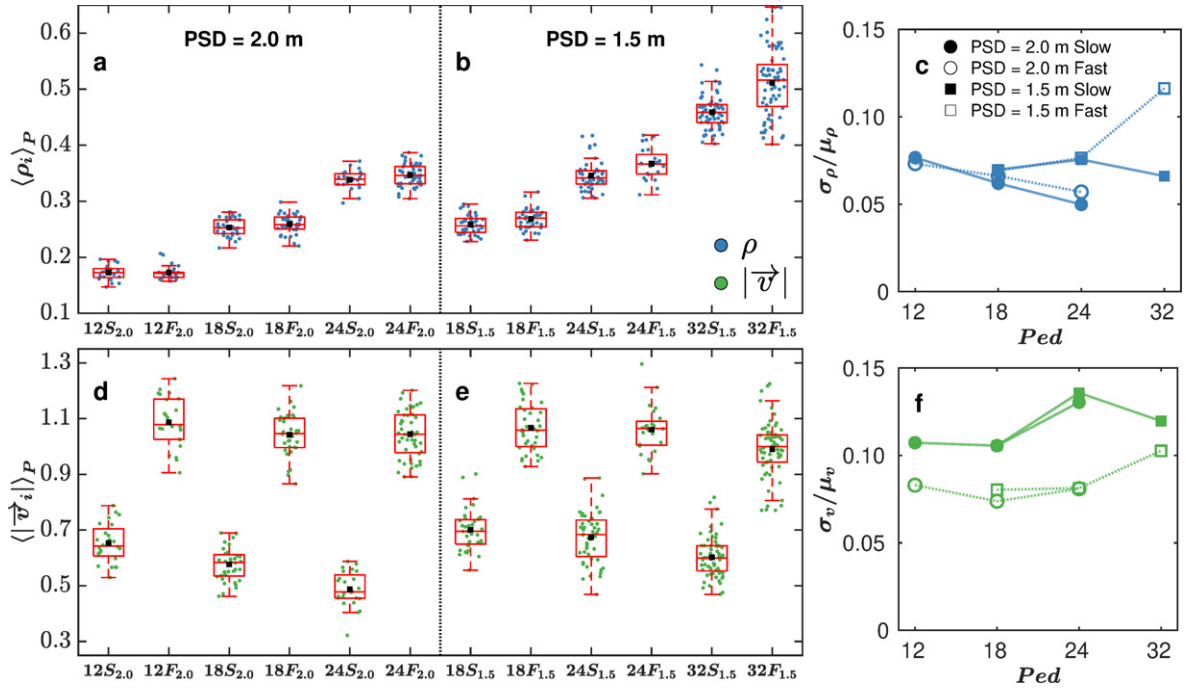

Figure 6. Boxplots and relative standard desviation (RSD) of $\langle \rho_i \rangle_P$ (blue color) and $\langle |\vec{v}_i| \rangle_P$ (green color) for all experiments. (a), (b) Boxplots of individual density values for a PSD of 2.0 and 1.5 m respectively. (d), (e) The same but for the individual speed values. Each point on the graphs represents the average value of ρ_i or $|\vec{v}_i|$ distributions for each individual. Thus, a mean value of density $\langle \rho_i \rangle_P$ and velocity $\langle |\vec{v}_i| \rangle_P$ per person are obtained. Black dots represent the average of the whole set of points. Red boxes display the median and the interquartile range (IQR), and the whiskers reach the closest data point inside the 1.5 IQR. (c), (f) RSD is calculated for the four distinct global densities and the different experimental conditions explored (see legend).

the only difference occurs in the 32 pedestrian case where the dispersion of the data in the fast case seems to be higher than in the slow one. In order to characterize in a better way the variability between pedestrians, the relative standard deviation values are shown in figure 6(c) for each experimental condition. They have been computed as σ/μ, where σ and μ are respectively the standard deviation and mean value of the data set $\langle \rho_i \rangle_P$ for each experiment. It is observed that the experimental conditions do not play a significant role in the variability among pedestrians except for the case with maximum global density (32 pedestrians) where the difference between fast and slow WS becomes noticeable as it was previously supposed.

Let us now consider the $\langle |\vec{v}_i| \rangle_P$ values in figures 5(d) and (e). For this case, the dispersion among the values obtained for each individual seems higher than the one observed for the density. Indeed, differences up to 25% between the fastest and slowest person for the same experiment can be found. Also, it seems that there is not any remarkable effect of the experimental conditions explored on the variability among different pedestrians. In order to check this, we follow the same procedure than for the density, and represent

the relative standard deviation values as a function of the number of pedestrians inside the arena (figure 6(f)). In this way, we clearly observe that the increase of the overall density does not produce important differences in terms of variability between pedestrians. On the contrary, the suggested WS has a highly noticeable effect: the highest relative standard deviations are systematically obtained in experiments with slow recommended WS. We speculate that this could be caused by the dissimilar interpretation that each pedestrian gives to the meaning of slow WS. Incidentally, the average values reported with black squares in figures 5(d) and (e) (recall that these are obtained by averaging the mean velocities of all pedestrians participating in the same experiment) reveal the expected behavior of a systematic speed decrease when augmenting the global density.

4. Conclusions

In this manuscript we have presented a detailed analysis of the speed–density relations found in lab experiments of pedestrians moving in a rectangular room while trying to keep a PSD. The first outright result is that in a situation in which the available space is rather large, the local density only affects the pedestrian speed in a weak manner: increasing the density leads to a slight reduction of the observed speed. On the contrary, we observe an important dependence of the speed–density relation on the specific experimental condition. In particular, we find that for the range of low densities used in our experiments, motivation (in the sense of choosing a fast or slow WS) primarily determines the speed–density curve that is obtained. In addition, we observe that the global density (given by the number of pedestrians in the arena) has a noticeable effect in the speed–density relations, especially when the stipulated WS is low and the PSD is large. This can be explained if we consider that, in these circumstances, the number of conflicts among pedestrians in terms of close approaches is minimized. Therefore, pedestrians have enough time to decide their direction taking into account not just their first neighbors, but also their perception of the rest of the room.

In another vein, the outcomes obtained when constructing the speed–density relation for each pedestrian separately, reveal a rather high variability among the individuals. This variability, which appears to be slightly more important in the pedestrians velocities than in the established densities, implies that each person has their own speed–density relation. It is nice to confirm that those pedestrians who moved faster in low-density conditions maintained the same attitude when the density increased; the same occurs for slower pedestrians.

Finally, let us stress once more that this experimental system is obviously an idealisation of a real system. Hence the need to take certain precautions when extrapolating these results to situations closer to the real world. However, we believe that this work can be considered as a good starting point for either the design of new experiments or the validation of new numerical models that aim to simulate pedestrian behavior in the new social scenario imposed by the COVID-19 outbreak.

Acknowledgments

We thank L F Urrea for his technical support and all the volunteers for their unselfish collaboration. I E, A G, R C H and I Z acknowledge support by Spanish Government Project FIS2017-84631-P, MINECO/AEI/FEDER, UE. D R P acknowledges financial support from Grant PID2015-003 ANPCyT (Argentina). I E acknowledges Asociación de Amigos, Universidad de Navarra, for his Grant.

References

[1] Helbing D, Farkas I and Vicsek T 2000 *Nature* **407** 487–90
[2] Buchanan A H 2001 *Fire Engineering Design Guide* (Canterbury: Centre for Advanced Engineering, University of Canterbury)
[3] Daamen W and Hoogendoorn S P 2012 *Fire Technol.* **48** 55–71
[4] Garcimartín A, Parisi D R, Pastor J M, Martín-Gómez C and Zuriguel I 2016 *J. Stat. Mech.* 043402
[5] Greenberg H 1959 *Oper. Res.* **7** 79–85
[6] Seyfried A, Steffen B, Klingsch W and Boltes M 2005 *J. Stat. Mech.* P10002
[7] Seyfried A, Steffen B and Lippert T 2006 *Physica* B **368** 232–8
[8] Chattaraj U, Seyfried A and Chakroborty P 2009 *Adv. Complex Syst.* **12** 393–405
[9] Zhang J 2012 *Pedestrian Fundamental Diagrams: Comparative Analysis of Experiments in Different Geometries* vol 14 (Jülich: Universität Wuppertal)
[10] Aghamohammadi R and Laval J A 2018 *Transp. Res.* B **38** 380
[11] Bosina E 2018 *A New Generic Approach to the Pedestrian Fundamental Diagram* vol 183 (Zurich: ETH Zurich) (https://doi.org/10.3929/ethz-b-000296226)
[12] Buchmüller S and Weidmann U 2006 Parameters of pedestrians, pedestrian traffic and walking facilities *Technical Report* Institut für Verkehrsplanung und Transportsysteme (https://doi.org/10.3929/ethz-b-000047950)
[13] Hankin B D and Wright R A 1958 *J. Oper. Res. Soc.* **9** 81–8
[14] Older S 1968 *Traffic Eng. Control* **10** 160
[15] Mōri M and Tsukaguchi H 1987 *Transp. Res.* A **21** 223–34
[16] Weidmann U 1993 Transporttechnik der fussgänger. Transporttechnische eigenschaften des fussgängerverkehrs, literaturauswertung *Technical Report* Institut für Verkehrsplanung, Transporttechnik, Strassen- und Eisenbahnbau (https://doi.org/10.3929/ethz-a-000687810)
[17] Helbing D, Johansson A and Al-Abideen H Z 2007 *Phys. Rev.* E **75** 046109
[18] Jin C J, Jiang R, Wong S, Li D, Guo N and Wang W 2017 arXiv:1710.10263
[19] Lohner R, Muhamad B, Dambalmath P and Haug E 2018 *Collec. Dyn.* **2** 1–15
[20] Navin F P and Wheeler R J 1969 *Pedestrian Flow Characteristics* vol 19 (Washington, DC: National Academies of Sciences, Engineering, and Medicine)
[21] Fruin J J 1971 Pedestrian planning and design *Technical Report*
[22] Tanaboriboon Y and Guyano J A 1989 *ITE J.* **59** 39–41
[23] Virkler M R and Elayadath S 1994 *Pedestrian Speed-Flow-Density Relationships HS-042 012*
[24] Parisi D R *et al* 2020 arXiv:2009.04019
[25] Mayr C M and Köster G 2020 arXiv:2007.01634
[26] Pouw C A S, Toschi F, van Schadewijk F and Corbetta A 2020 *PLoS One* **15** e0240963
[27] Echeverría-Huarte I, Garcimartín A, Hidalgo R, Martín-Gómez C and Zuriguel I 2021 *Sci. Rep.* **11** 1534